# Mechanical performance of vegetal fabric reinforced cementitious matrix (FRCM) composites

**Luis Mercedes [(1)], Lluis Gil [(2)], Ernest Bernat-Maso [(2)]**

[(1)] Department Strength of Materials, Polytechnic University of Catalonia, Terrassa, Spain

[(2)] LITEM Laboratory for Technological Innovation of Structures and Materials, Spain

Abstract

In order to pursue sustainable objectives in the construction industry, a new composite material using vegetal fibre mesh coated with resin and embedded in mortar is developed and characterized. In this study, meshes of different types of vegetal fibres (flax, hemp, sisal, and cotton) coated with epoxy and polyester resins were manufactured. A mixture of meshes and mortar cast different fabric-reinforced cementitious matrix (FRCM) specimens, which were later subjected to direct tensile tests. The results showed an excellent interaction between the vegetal fibres and the mortar matrix. The coating with epoxy and polyester improved the mechanical properties of the yarns and apparently avoided the typical slipping failures in FRCM composites. Hemp and flax FRCM are the composites that reached the highest mechanical strength, whereas cotton FRCM had the greatest elongation capacity and multicracking response. In addition, an analytical model was proposed and validated by a comparison with the experimental results.

**Keywords**: Cementitious matrix, Vegetal fibres, FRCM

## 1. Introduction

Fabric-reinforced cementitious matrix (FRCM) composites emerged as a promising alternative to organic matrix based fibre reinforced polymers (FRPs) because of their simple workability, significant fire resistance, and ability to dissipate energy through developing multicracking patterns under cyclic loads, among other advantages [1]. Thus, FRCM composite is a feasible option for the strengthening of structures [2][3][4][5]. FRCM consists of a mesh embedded in an inorganic mortar matrix. This mesh can be made of diverse materials such as glass fibre, carbon fibre, basalt fibre, PBO (Polyparaphenylene benzobisoxazole), and vegetal fibre [6].

It is essential to understand that FRCM provides tensile strength thanks to the fibres of the meshes, and that these fibres only bear the loads that the mortar is capable of transmitting [1]. Therefore, the transmission of matrix-mesh stresses is one of the main requirements to be considered, as well as the geometric adaptability of the mesh and its chemical stability (durability) within the matrix.

If the structure-matrix adhesion is not sufficient, a failure of the reinforced structure tends to be produced by debonding of the FRCM composite [7]. When the interface structure matrix and the matrix-fibre connection work correctly, a failure can be observed owing to exhaustion of the tensile strength of the mesh [2]. However, it is important to point out that when the masonry is subjected to eccentric loads, Cevallos et al. [8] showed that the strength of the composite material (mortar fibres) is not the only decisive factor in the behaviour of masonry walls, since a greater rigidity of the mesh can lead to failure by detachment of the FRCM.

The low cost, low density, recyclability, and biodegradability characteristics of vegetal fibres make them a sustainable alternative to synthetic fibres commonly used in FRCM. In terms of strength capacity, the use of these fibres is limited by their low mechanical properties compared with synthetic ones [9]. However, the low cost and low density of vegetal fibres make it possible to use a greater volume. Thus, there is a challenge in developing composite materials with mechanical properties comparable to those made of synthetic fibres. A study published by Wambua et al. [10], where the mechanical properties of natural fibres (organic matrix) composites compare favourably with

properties corresponding to glass fibre composites, is an example of the possibilities of natural fibres.

On the other hand, the organic origin of vegetal fibres favours their degradation in the environment of cementitious matrix composites [11] owing to high alkalinity and humidity cycles. In view of this drawback, some authors have studied the feasibility of applying treatments to avoid the degradation of the fibres. One of these treatments is the coating of fibres with a resin [12].

Coating the fibre with resin affects the sustainability (increasing its cost and exhibiting toxicity) of the vegetal fibres. However, nowadays, the coating on commercial meshes to use in FRCM composites is a widely used technique. In some cases, this avoids the fibre degradation within the cementitious matrix [13], and in other cases, it improves the mechanical properties and the bond of the meshes with the matrix [14][15].

For vegetal fibre meshes, using a coating is justified for the substitution of synthetic fibres, the protection of the fibre in an aggressive cementitious matrix, and improving the mechanical and mesh-matrix interaction. Although using resin to coat fibres is not environmentally friendly, the proposed substitution of synthetic fibres by vegetal fibres is a steps forward in this line.

Nowadays, there are some studies [16][17][18][19] which analyse the behaviour of vegetal fibres within FRCM composites. These studies demonstrate the great potential of vegetal fibres as reinforcement. One of these studies was presented by Menna et al. [16], who, with the objective of using vegetable fibres with the best efficiency within an FRCM, studied an innovative FRCM system with hemp meshes impregnated with epoxy resin. The results showed that the impregnation of hemp yarns with a flexible epoxy resin allowed for better exploitation of the tensile properties of the hemp fibres. In addition, the reinforcement of masonry walls using FRCM with a hemp mesh impregnated with epoxy increased the shear strength by a factor of 2–3 in the case of masonry walls of tuff and by about 5 in the case of walls of clay masonry. However, the influence of resin coatings on other vegetal fibre yarns and the effect over manufactured FRCM composites still requires research.

In the case of an FRCM specimen subjected to a tensile test, there are many studies [15][20][21][22] that analysed their traction behaviour. Two of the most used test setups were the “clamped system,” which uses friction for load application realized by applying a compressive force normal to the plane of the specimen at its ends, and the “clevis grip,” in which the transfer mechanism between the specimen and the grip is by adhesive tension and shear realized through metal plates glued to the ends of the specimen.

The clevis grip was the choice for this study because it reproduces the behaviour that FRCM materials present in the field. Thus, it allows for the slipping of mesh, contrary to a climbed system, where mesh slipping is limited by the compression of the clamps.

In addition, considering that most studies about FRCM used fibres with a greater modulus of elasticity than mortar [23][24][15], it is important to analyse and identify how the use of fibres with a lower modulus of elasticity than mortar can influence the behaviour of FRCM. Moreover, it is necessary to propose an analytical model to predict the behaviour of FRCM in these cases.

With this aim, meshes with yarns of vegetal fibres coated with resin were designed, manufactured, and used to produce FRCM specimens, which were subjected to tensile tests. The behaviour of the tested FRCM specimens with different types of fibres was studied and used to validate an analytical model.

The article presents innovative and sustainable composites of cementitious matrix and vegetal fibres as an alternative to strengthen structures, through the use of a greater

quantity of fibres. This article also proposes analytical models that are useful in estimating this composite's behaviour.

## 2. Materials and manufacturing specimens

### 2.1. Vegetal fibre meshes

In order to obtain meshes of vegetal fibres with a load capacity comparable to that of synthetic fibre meshes, vegetal fibre meshes were designed (see Figure 1a) using as a reference the geometry of commercial mesh used in FRCM in other studies [6]. To achieve these load capacities, meshes with greater thickness (greater volume of fibres) than the commercial meshes of synthetic fibres were designed. This design should maintain enough spacing between tufts to assure an efficient interaction with the matrix.

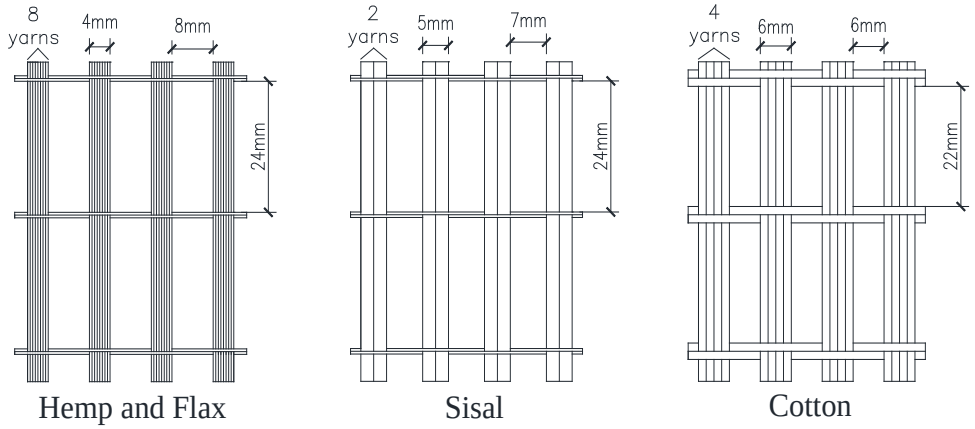


(a)

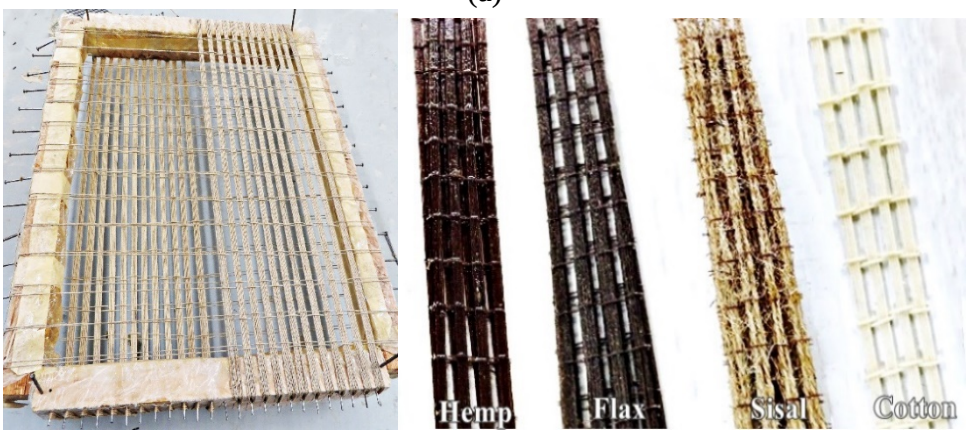


(b)

**Figure 1.** Design (a) and manufacturing (b) of vegetal fibre meshes

Meshes were made with hemp, flax, sisal, and cotton yarns. A wooden rectangular support as a hand loom was assembled to manufacture these meshes. The support was 200 × 600 mm and had nails at its external boundaries (Figure 1b). Nails were positioned 12 mm in the warp direction and 25 mm in the weft direction. These were useful for stretching and anchoring the yarns, making it possible to weave the meshes. Since yarns of different fibres were of different diameters, the number of yarns used in each tuft was different for each type of mesh. Weft yarns of sisal mesh were made of hemp in order to reduce the thickness of the weft and wrap crossing point since using the same number of yarn in all meshes would significantly increase the volume of mesh and the stiffness of some meshes (sisal and cotton).

Once the meshes were weaved, they were coated with a brush with resin. This created a superficial thin coat on the mesh. After one day of curing, meshes were cut into pieces of 40 × 390 mm.

Table 1 lists some properties of the yarns and meshes used. The diameter of the yarns was supplied by the manufacturer and confirmed with a digital caliper, carefully measuring the thickness when the yarn was stretched and avoiding yarn deformation. The diameter values made it possible to determine the yarn sections and mesh sections. Then, to determine the yarns' linear densities and volumetric densities, specimens of yarn of 40 cm were cut and then weighed on a precision scale.

**Table 1.** Properties of yarns and meshes

| Properties | Hemp | Flax | Sisal | Cotton |
|---|---|---|---|---|
| **Yarn diameter (mm)** | 0.5 | 0.5 | 2.5 | 1.5 |
| **Number of yarn/tuft** | 8 | 8 | 2 | 4 |
| **Yarn linear density (g/m)** | 0.40 | 0.43 | 3.63 | 1.20 |
| **Yarn volumetric density (g/cm$^3$)** | 2.04 | 2.17 | 0.74 | 0.67 |
| **Mesh weight/area (g/cm$^2$)** | 0.034 | 0.036 | 0.07 | 0.054 |

The epoxy resin used to coat the yarns was a low-viscosity and high-adhesion resin. In the case of polyester, the coating was a mix of a standard polyester to produce FRP laminates and a low-viscosity, low-reactivity, flexible, unsaturated polyester included to reduce the stiffness of the coating and to reduce its viscosity and workability. These two polyesters were mixed at a ratio of 50%. The mechanical properties of these resins are presented in Table 2. These numbers were provided by the supplier.

**Table 2.** Mechanical properties of resins

| Properties | Epoxy | Polyester | Flexible Polyester |
|---|---|---|---|
| Density (g/cm$^3$): | 1.05 | - | 1,2 |
| Tensile strength (MPa): | 22.9 ± 4 | 69.6 | 15 |
| Elongation (%): | 18.2 ± 7 | 1.9 | 50 |
| Flexural strength (MPa): | No break | 138.6 | 10 |
| Flexural modulus (MPa): | 233.1 | 4095 | 220 |

Fifteen specimens were prepared for each type of yarn to study the mechanical response under tensile efforts. Five specimens were coated with epoxy, five were coated with polyester, and five were not coated. A sheet of glass FRP was fabricated at each end of every yarn specimen, embedding it. These glass FRP sheets were used as clamping surfaces which assured the correct stress transmission from the testing system to the yarn (Figure 2).

**Figure 2.** Preparation of glass-FRP sheet at ends of yarn specimens prior to test

## 2.2. FRCM specimens

twenty-four FRCM specimens were produced with meshes and three without mesh (only mortar). Wood moulds were prepared to manufacture 10 × 50 × 400-mm specimens. The production procedure consisted of the following steps: a) placing the first layer of mortar in a mould of approximately 5-mm thickness, b) placing the mesh so it slightly penetrated this first layer of mortar, and c) placing the second layer of mortar to reach a total thickness of 10 mm (Figure 3). After seven days of curing, specimens were demoulded and left for curing. During the curing process, four metal plates were bonded at their ends (one on each side) by means of an epoxy bicomponent adhesive. The purpose of these metal plates was to facilitate a connection with the testing system. The length of the plates bonded to the specimen was 100 mm (used in other studies [25][26]) at each end.

Control mortar specimens measuring 40 × 40 × 160 mm were taken during the production of specimens to determine the flexural and compressive mortar strength at 28 days of curing.

**Figure 3.** Manufacturing of FRCM specimens

To prepare the specimens, a single-component thixotropic mortar based on cement and synthetic resins, including silica fume and reinforced with polyamide fibres, was used. This mortar complies with the requirements of type R3 as defined in UNE-EN 1504-3 [27].

The control mortar specimens were tested to flexion in an electromechanical press of 50 kN, and then the resulting halves were tested under compression with an hydraulic actuator of 100-kN capacity. These tests were performed according to EN 1015-11: 2000 [28]. The averaged results of the compression and bending tests and other mechanical properties (supplied by the manufacturer) are summarized in Table 3.

**Table 3.** Properties of mortar

| | |
|---|---|
| **Chemical composition (1)** | Prepared cement mortar, improved with synthetic resins and silica fume, and reinforced with polyamide fibres |
| **Density of fresh Mortar (1):** | 2.1 kg/l (a + 20ºC). |
| **Granulometry (1):** | 0–2 mm |
| **Compressive Strength (2):** | 39.25 MPa |
| **Flexural Strength (2):** | 6.56 MPa |
| **Tensile Strength (2):** | 2.9 MPa |

(1) Supplied by manufacturer; (2) results of test (EN 1015-11: 2000)

## 3. Tensile test setup

### 3.1. Yarns

Yarn specimens with and without resin were tested based on code EN ISO 13934-1/2 [29] but were adapted to the particular requirement. These were tested in an electromechanical press with a maximum load capacity of 10 kN. A preload of 5 N was applied prior to the test to ensure alignment of the fibre and to have it straight enough to install an extensometer of 25-mm range to measure deformations on an initial length of 50 mm (see Figure 4). The test rate was set at 5 mm/min.

**Figure 4.** Yarn tensile test

3.2. FRCM

FRCM specimens were tested following the procedure described in AC434-0213-R1 [30] at 28 days of curing. The specimens were totally hinged at both ends, and the electromechanical press was used to apply an imposed elongation of 5 mm/min. Deformations were measured with the same extensometer of 25-mm range used in yarn testing, but in this case it was attached to a system formed for two 'L' steel pieces. These steel pieces were adjoined by magnets to the edge of the connection plates (see Figure 5). Thus, the base length for the strain measurements was 200 mm.

**Figure 5.** FRCM tensile test

## 4. Results and Discussions

4.1. Experimental results of vegetal fibre yarns

Yarns with coating and without coating were produced and tested in order to obtain their tensile strength and mechanical response. The tests were also useful in analysing the effect of the resins on the structural response of vegetal yarns.

Table 4 lists some properties of the yarns and meshes that were coated. Yarns of 40 cm in length with coating were weighed on a precision scale before endings that clamped the glass FRP sheets were fabricated. The yarns were stretched and coated with a brush

until their entire external surface was coated. This was done to quantify the amount of resin applied to each yarn, and thus to estimate the amount of resin needed to coat the meshes. The linear density of the yarns with coating was calculated to determine the quantity of resin applied per yarn length and the expected mesh weight.

**Table 4.** Yarns properties and quantification of resin applied

| Properties | Hemp | Flax | Sisal | Cotton |
|---|---|---|---|---|
| Yarn + epoxy linear density (g/m) | 0.89 | 0.92 | 8.14 | 4.13 |
| Epoxy/yarn length (g/m) | 0.5 | 0.5 | 4.51 | 2.93 |
| Epoxy/mesh area (g/cm$^2$) | 0.015 | 0.016 | 0.03 | 0.05 |
| Mesh + epoxy weight/area (g/cm$^2$) | 0.075 | 0.077 | 0.217 | 0.189 |
| Yarn + polyester linear density (g/m) | 1.18 | 1.28 | 9.36 | 4.70 |
| Polyester/yarn length (g/m) | 0.78 | 0.85 | 5.73 | 3.5 |
| Polyester/mesh area (g/cm$^2$) | 0.02 | 0.03 | 0.04 | 0.06 |
| Mesh + polyester weight/mesh area (g/cm$^2$) | 0.099 | 0.107 | 0.25 | 0.215 |

For hemp and flax, the amount of resin applied is very similar, since their thicknesses are the same and the absorption capacity of both cases (according to bibliography [10]) is very similar. However, more resin was applied to the sisal and cotton yarns because these are thicker (sisal: 2.5 mm and cotton: 1.5 mm).

Regarding the meshes, more resin was used on the cotton meshes than the sisal ones. This is because both the weft and wrap of the cotton meshes were made of cotton yarn, whereas the weft yarns of sisal mesh were made of hemp in order to reduce the thickness of the weft-wrap crossing point, as explained previously.

Comparing the yarns coated with epoxy with the yarns coated with polyester, it is observed (see Table 4) that the yarns with polyester have a higher weight of resin. This is mostly owing to the higher density of the polyester in comparison with the epoxy used (epoxy: 1.02 g/cm$^3$ and polyester: 1.2 g/cm$^3$).

Table 5 lists the mean values of the tensile strength and the modulus of elasticity for each yarn. The stresses were calculated considering the yarn diameter (Table 1), and the modulus of elasticity was calculated considering the linear part of 15 and 85% of $\sigma_{Yarn}$ in the stress-strain diagram of hemp, flax, and sisal, and of 30 and 85% of $\sigma_{Yarn}$ in the stress-strain diagram of cotton (Figure 8).

**Table 5.** Results of tensile tests of yarns

| Mechanical properties of yarns | | | | | | | | | | | | |
|---|---|---|---|---|---|---|---|---|---|---|---|---|
| **Yarns** | **Without Resin** | | | | **With Epoxy** | | | | **With Polyester** | | | |
| | Hemp | Flax | Sisal | Cotton | Hemp | Flax | Sisal | Cotton | Hemp | Flax | Sisal | Cotton |
| **No. of test** | 5 | 5 | 5 | 5 | 5 | 5 | 5 | 5 | 5 | 5 | 5 | 5 |
| **$F_{Yarn}$ (N)** | 58.00 | 81.80 | 475.20 | 95.20 | 102.2 | 123.80 | 546.80 | 162.40 | 106.80 | 101.41 | 453.00 | 145.60 |
| **$\sigma_{Yarn}$ (MPa)** | 295.54 | 416.82 | 96.86 | 53.90 | 520.76 | 630.83 | 111.45 | 91.95 | 544.20 | 516.72 | 92.33 | 82.43 |
| **(C.V)** | (11%) | (17%) | (9%) | (1%) | (7%) | (9%) | (8%) | (1%) | (7%) | (6%) | (12%) | (6%) |
| **$\varepsilon_{Yarn}$ (%)** | 1.03 | 1.65 | 3.01 | 10.19 | 1.30 | 1.66 | 2.15 | 7.81 | 0.98 | 1.29 | 2.61 | 7.13 |
| **(C.V )** | (15%) | (18%) | (11%) | (5%) | (14%) | (11%) | (8%) | (5%) | (14%) | (12%) | (5%) | (12%) |
| **$E_{Yarn}$ (GPa)** | 26.33 | 24.98 | 3.75 | 0.53 | 38.74 | 36.01 | 4.87 | 0.93 | 50.58 | 37.95 | 3.78 | 0.88 |
| **(C.V )** | (4%) | (8%) | (6%) | (6%) | (6%) | (12%) | (12%) | (4%) | (15%) | (10%) | (8%) | (2%) |

(C.V) = coefficient of variation, $F_{Yarn}$ = maximum load mean, $\sigma_{Yarn}$ = tensile strength mean, $\varepsilon_{Yarn}$ = deformation peak mean, $E_{Yarn}$ = Young's modulus mean

The results presented in Table 5 show that the noncoated vegetal fibre yarn that presented the highest strength was flax, followed by hemp, sisal, and cotton. The

modulus of elasticity of the hemp yarn is slightly higher than that of flax yarn, but these two values are significantly higher than the modulus of elasticity of sisal and cotton yarns. In addition, it can be seen that the yarn with the highest elongation capacity is the cotton yarn, followed by sisal, flax, and hemp.

Comparing the tensile response of vegetal fibre yarns with the tensile response of some synthetic fibres presented in other studies [15], it can be seen that the tensile strength and modulus of elasticity are higher in the case of synthetic fibres. Thus, producing tufts with several yarns of vegetal fibres was necessary to achieve a comparable load capacity through the use of a greater amount of fibres owing to low cost, low density, and the sustainable alternative that it represents.

The results presented in Table 5 show that the coatings increased the tensile strength (except for sisal yarn coated with polyester) and stiffness of vegetal fibre yarns. The percentage of increase in the tensile strength and Young's modulus are presented in Figure 6.

The vegetal yarn that was most affected by the coating was the hemp yarn with polyester, which reached an 84% increase in the tensile strength and a 92% increase in Young's modulus. A similar tendency was observed for the hemp yarns with epoxy (76 and 47% increases in the tensile strength and Young's modulus, respectively).

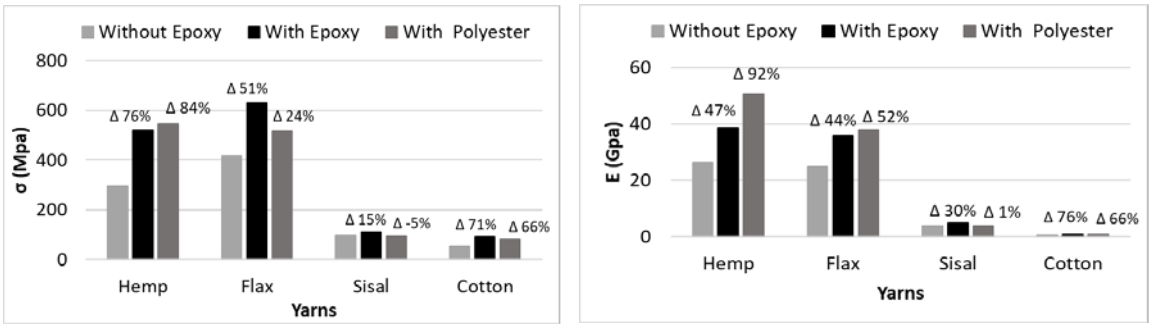


(a) (b)

**Figure 6.** Influence of coating on tensile mechanical response of yarns: (a) tensile strength, (b) Young's modulus

However, the tensile strength of sisal yarn seems to decrease when these were coated with polyester. The modulus of elasticity showed a slight increase (1%) in this case. By contrast, both the tensile strength (15%) and modulus of elasticity (30%) increased when sisal yarns were coated with epoxy. Taking into account that sisal is the yarn with the greatest diameter (2.5 mm), it is more difficult for the resin to penetrate the internal structure of these yarns. This might be of special significance in the case of the polyester coating, which had a lower fluidity than the epoxy one.

Thus, it is observed that the influence of the resin on the mechanical response of vegetal yarns depends mostly on the ability of the resin to penetrate the internal structure of the yarn, which in turn depends on the structure and diameter of the yarn.

Figure 7 shows the stress-strain diagrams for the coated and noncoated yarns. These graphs help to understand the results presented in Table 5 and make the influence of the coating on the tensile strength and Young's modulus evident.

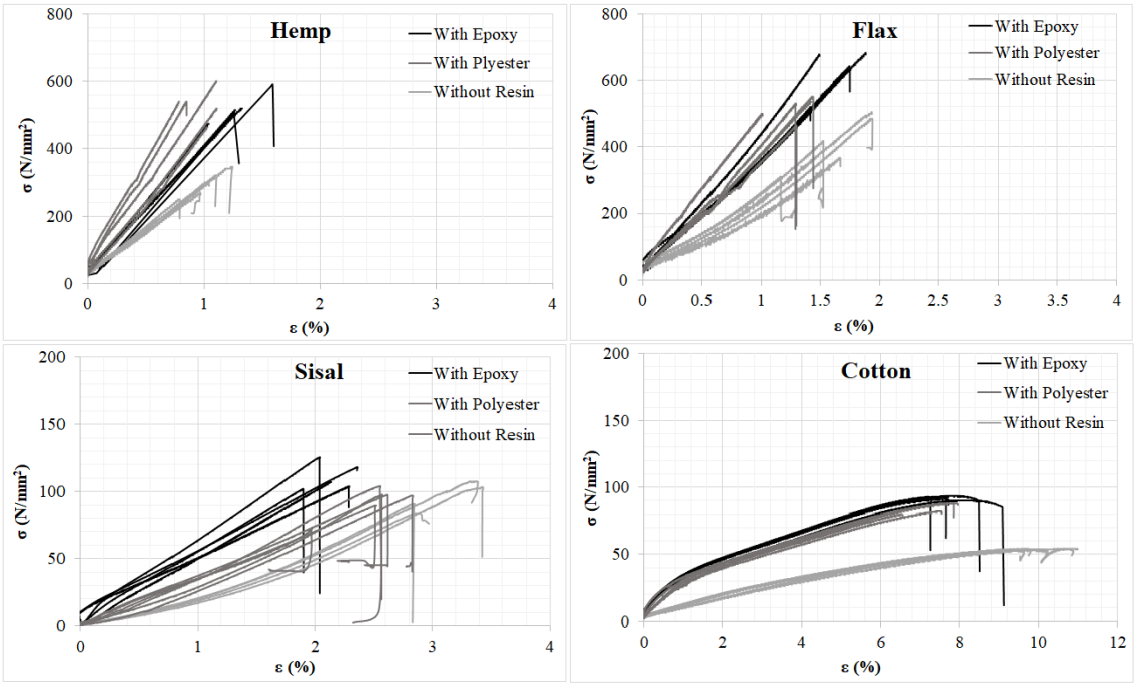


**Figure 7.** Stress-strain diagrams for tested yarns

The results show the great influence of coating the yarns of vegetal fibres with resin. However, it is necessary to use mechanized methods of coating in order to avoid adding excessive resin and to determine the optimal application of resin. In addition, using more sustainable resin (eco green resin) should be considered to follow the environmental friendly purpose of vegetal fibres.

4.2. Experimental results of FRCM4.2.1. Failure modes

Two failure modes were observed in the tensile test of the FRCM specimen: mortar deboning and mesh rupture (see Figure 8).

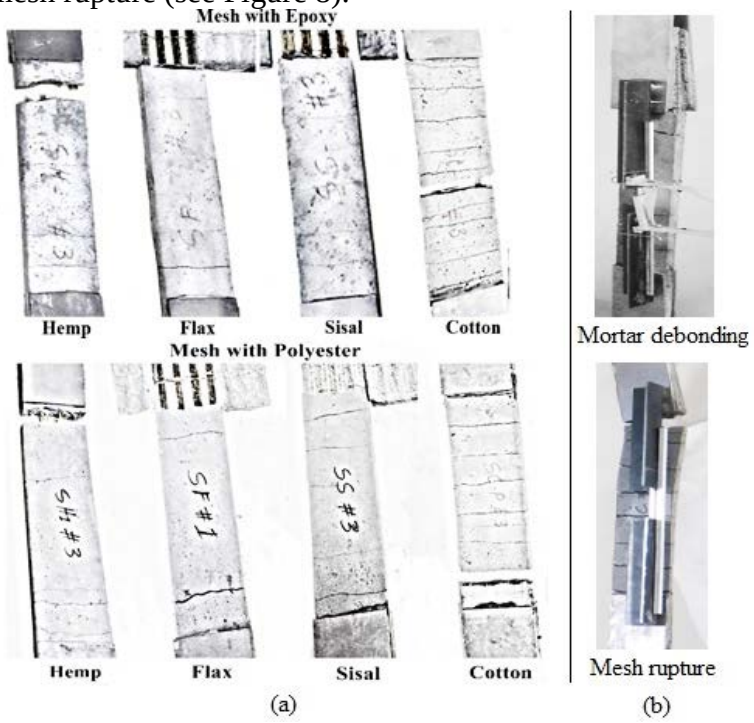


**Figure 8.** Failures of FRCM in tension: (a) mesh with epoxy and polyester, (b) failure modes

Mesh rupture failure: This occurred in some specimens of hemp, flax, and cotton. This mode of failure was not common in specimens with synthetic meshes tested with the clevis grid system in other studies [31][25] (where slipping mesh failure is common). This is perhaps owing to the fact that the coating improved the adherence of the mesh within the matrix [14], thus avoiding the failure of slipping of mesh. This mode of failure indicates a greater use of the tensile capacity of these vegetal fibre yarns.

Mortar debonding failure: This was present in all sisal specimens, and in some specimens of hemp, flax, and cotton. The authors believe that this mode of failure (not commonly seen in other studies which used the clevis system) is associated with the attempt to slip the mesh and the greater thickness of mesh used in this study because this section of mortar is not capable of allowing the slipping of mesh with such thickness (sisal: 2.5 mm). This failure mode can also be influenced by the bonded length (100 mm) because some studies [22][14] demonstrated that this affects the tension behaviour of FRCM composites. These studies suggested a bonded length of 150 mm for a specimen with similar dimensions to those used in this study.

In the case of FRCM with mesh coated with polyester, mortar debonding failure was more present. This may be because the bond with the matrix provided by the polyester was weaker than that of the mesh coated with epoxy.

The number of cracks developed in the vegetal-fibre FRCMs depended on the mechanical properties of the coated fibre meshes and the thickness of these meshes. Hemp, flax, and sisal FRCMs showed a stiffer response than those of cotton. This is consistent with the stiffer behaviour of the coated yarns presented in Figure 4. Yarn tensile test. These cases developed between three and six cracks. By contrast, cotton FRCM developed between 7 and 18 cracks (more cracks were observed in the cases with epoxy-coated cotton mesh), verifying the proper mesh-matrix interaction which allowed use of the elongation capacity of the cotton yarns.

4.2.2. Mechanical Properties of FRCM

The results obtained from the tensile tests of the FRCM specimens are listed in Table 6. This shows the ultimate stress ($\sigma_{Mesh}$) calculated using the cross-sectional area of the mesh (determined from the yarn diameters, Table 1) because it was the mesh that absorbed the load when the mortar was cracked and the stress when the first crack started ($\sigma_{mc}$). This was calculated using the cross-sectional area of the FRCM specimens.

**Table 6.** Experimental results of FRCM

| **Mechanical Properties of FRCM** | | | | | | | | | |
|---|---|---|---|---|---|---|---|---|---|
| **FRCM** | | **Mesh with Epoxy** | | | | **Mesh with Polyester** | | | |
| | **Mortar without mesh** | **Hemp** | **Flax** | **Sisal** | **Cotton** | **Hemp** | **Flax** | **Sisal** | **Cotton** |
| **Number of tests** | 3 | 3 | 3 | 3 | 3 | 3 | 3 | 3 | 3 |
| **Mesh area** | - | 6.28 | 6.28 | 39.25 | 28.26 | 6.28 | 6.28 | 39.25 | 28.26 |
| **$\sigma_{mc}$** | 4.61 | 5.50 | 4.38 | 3.88 | 2.80 | 3.70 | 4.01 | 2.17 | 2.39 |
| **(MPa)** | (11%) | (1%) | (24%) | (10%) | (18%) | (6%) | (20%) | (5%) | (18%) |
| **$F_u$** | 2303 | 3481 | 2615 | 3697 | 2711 | 2985 | 2757 | 1684 | 2172 |
| **(N)** | (11%) | (14%) | (11%) | (8%) | (5%) | (11%) | (11%) | (36%) | (2%) |
| **$\sigma_{Mesh}$** | - | 554.25 | 416.35 | 94.18 | 95.94 | 475.3 | 438.93 | 42.9 | 76.86 |
| **(MPa)** | | (14%) | (11%) | (8%) | (5%) | (11%) | (11%) | (36%) | (2%) |

| | | | | | | | | | |
|---|---|---|---|---|---|---|---|---|---|
| $\sigma_{Mesch}/\sigma_{Yarn}$ (%) | - | 106.3 | 66 | 84.51 | 104.34 | 87.34 | 84.95 | 46.46 | 93.23 |
| $E_I$ | 8.92 | 21.5 | 13.73 | 16.74 | 6.22 | 13.03 | 9.78 | 8.7 | 6.55 |
| (GPa) | (40%) | (20%) | (20%) | (60%) | (27%) | (38%) | (37%) | - | (40%) |
| $E_{II}$ | - | 99.52 | 58.92 | 18.34 | 6.02 | 42.2 | 51.75 | 2.29 | 9.38 |
| (GPa) | | (12%) | (38%) | (19%) | (47%) | (16%) | (18%) | (33%) | (69%) |
| $E_{III}$ | - | 46.18 | 35.83 | 2.04 | 0.53 | 32.64 | 19.90 | 1.66 | 0.71 |
| (GPa) | | (22%) | (32%) | (31%) | (5%) | (12%) | (23%) | (33%) | (22%) |
| $\Delta E/E_{yarn}$ (%) | - | -19.20 | 0.50 | 58.11 | 43.01 | 35.47 | 47.56 | 56.08 | 19.32 |

(%) = coefficient of variation, $F_{um}$ = maximum load, $\sigma_{mc}$ = stress of first crack formation, $\sigma_{Mesch}/\sigma_{Yarn}$ = percentage of utilization of strength of yarns, $\Delta E/E_{yarn}$ (%) = damage index

In Table 6, it can be observed that the unreinforced mortar specimens presented an average tensile strength of 4.61 MPa, which is higher than the tensile strength indirectly calculated from the results of the flexural tests on the control (40 × 40 × 160 mm) mortar specimens (2.9 MPa).

The FRCM composite which showed the highest ultimate load was epoxy-coated sisal FRCM, followed by epoxy-coated hemp FRCM, polyester-coated hemp FRCM, polyester-coated flax FRCM, and epoxy-coated cotton FRCM. However, the highest stress on the mesh was observed in the epoxy-coated hemp FRCM, followed by the polyester-coated hemp FRCM and polyester-coated flax FRCM. The differences between the order of the ultimate load and the order of the mesh stresses are related with the different volumes of fibres used.

In Table 6, the percentage of utilization of the tensile strength of the yarns is included. This was calculated as the ratio of the mesh stress of the strengths of the yarns ($\sigma_{Mesh}/\sigma_{Yarn}$). It must be highlighted that all vegetal meshes in FRCM were coated, and thus, the ultimate tensile strength of the yarns to calculate the ratio corresponded to the coated yarns as well. The results showed that the epoxy-coated hemp FRCM presented the highest percentage of mechanical utilization of the fibres (106%, possibly owing to the variability of the experimental results), followed by cotton, sisal, and flax in the case of epoxy-coated meshes in FRCM. By contrast, the polyester-coated mesh which showed the greatest percentage of utilization inside the FRCM was polyester-coated cotton, followed by hemp, flax, and sisal in the case of polyester-coated meshes.

Comparing FRCMs including epoxy-coated meshes with FRCMs including polyester-coated meshes, it is observed that FRCMs with epoxy-coated meshes exhibited better performance than FRCMs with polyester-coated meshes. This indicates that the epoxy coating ensures better adhesion with a mortar matrix than polyester coating.

Two factors might have influenced the premature slip of the polyester-coated sisal: the greatest thickness of sisal mesh and the lower adhesion between polyester and the matrix in comparison with those of the epoxy coating.

Young's modulus presented in Table 6 were determined by considering the trilinear model presented by Aveston–Cooper–Kelly (ACK) [32][33]. Young's modulus was calculated for each state. This was calculated from the stress-strain diagram of FRCM shown in Figure 9. $E_I$ was calculated in the first slope from the stress-strain diagram (where there are no cracks) considering the tensile on the gross section of the specimens ($\sigma_{FRCM}$). $E_{II}$ was calculated in the first slope after the first crack of the mortar considering the tensile strength of the mesh section. $E_{III}$ was calculated in the last slope also considering the tensile strength of the mesh section.

$E_{II}$ and $E_{III}$ show a strong degradation of stiffness in the FRCM composites because of the mesh-matrix interaction in the second state of the trilinear model.

The damage index ($\Delta E/E_{yarns}$) in Table 6 was calculated for the variation between Young's modulus in stage III and Young's modulus of the yarns. This shows the damage accumulated in Young's modulus of yarns after the mesh-matrix interaction of stage II. In the case of FRCM of hemp and flax with epoxy, the modulus seems to have not been affected. However, the coefficients of variation in these specimens are very high (22 and 32%), so these values are not completely reliable.

Stress-strain diagrams of the tensile tests on the FRCM specimens are presented in Figure 9. To plot these graphs, the sectional areas of meshes (axis 'y' on the left) and the sectional area of FRCM (axis 'y' on the right) were considered to calculate the stress. This is because different behavioural states appear in the FRCM composites. The results show the multicracking behaviour of FRCM composites associated with the mesh-mortar interaction after the first cracking of the mortar. This multicracking behaviour is similar to that obtained by other studies [14], although in this study the mesh-mortar interaction is more remarkable.

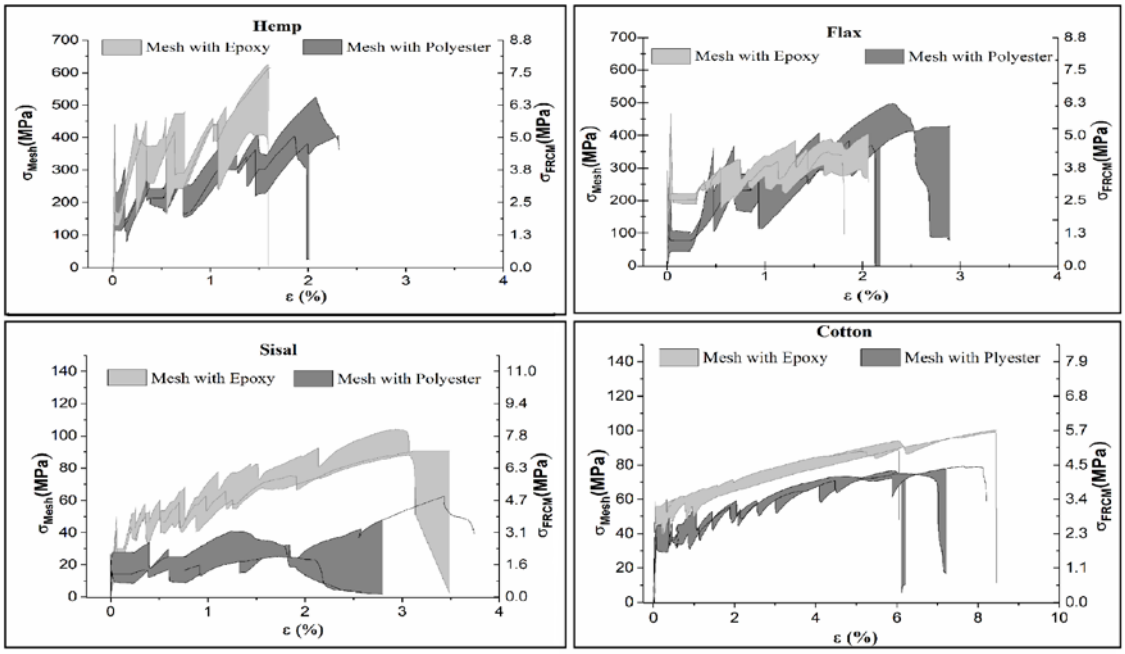


**Figure 9.** Experimental stress-strain diagrams of FRCM

## 5. Theoretical behaviour of FRCM

For a theoretical behaviour study of the FRCM with regard to traction, two models are commonly used: a bilinear model that is recommended to test with the clevis grips system [30], and a trilinear model recommended to test with the clamping system [32].

The difference between these two models is that the bilinear model superimposes two behaviour states and ignores the mesh-mortar interaction after the first crack of the mortar. This model considers that all tensions are absolved by the mesh after the first crack of the mortar, while the trilinear model considers this state of the mesh-mortar interaction (crack formation).

In this study, the trilinear model presented by ACK [32][33] was used because the stress-strain diagrams show a clear stage of mesh-mortar interaction (perhaps owing to improvements in the bond mesh-matrix by the coating of mesh). The authors believe that this must not be ignored.

The ACK theory consists of a trilinear definition which superimposes the experimental stress-strain curve of FRCM systems. These three lines represent three different behaviour stages (see Figure 10) that can be identified as follows:
I: First elastic-linear stage without cracks, where mortar and mesh deform together,
II: Stage of crack formation, characterized by the multicracking of mortar induced by the mesh-mortar interaction along the specimen, and
III: Cracking stabilization, where all stresses are borne by the mesh.
The assumptions employed in the development of the ACK theory are as follows:

- ✓ The fibres are only capable of carrying a load along their longitudinal axes.
- ✓ The matrix-fibre bond is weak.
- ✓ Once the matrix and the fibre debond, a pure frictional shear stress rules the matrix-fibre interface behaviour.
- ✓ The frictional interface shear stress is constant along the debonded interface.
- ✓ The Poisson effects of the fibre and matrix are neglected.
- ✓ Global load sharing is assumed for the fibres.
- ✓ Normal matrix stresses, transversal to the loading direction, are uniform in a cross section.

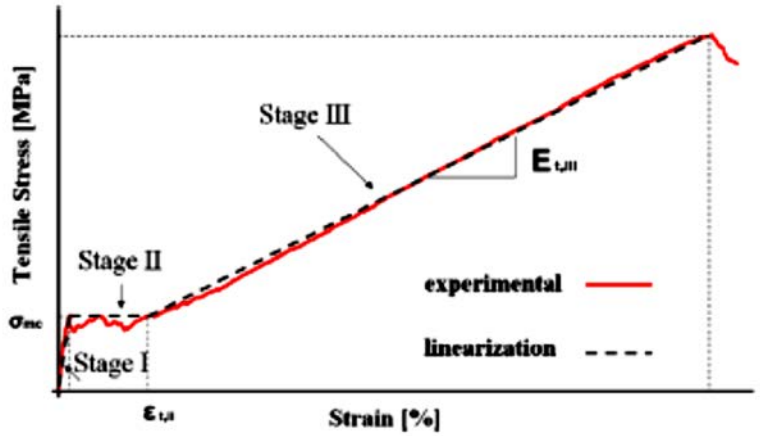


**Figure 10.** Typical stress-strain curve of FRCM in tension and ACK model [33]

According to the ACK theory, in the first stage, FRCM obeys the law of mixtures.

$$E_I = E_f V_f + V_m E_m \quad (1)$$

where $E_I$ is Young's modulus of FRCM in stage I, $E_f$ represents Young's modulus of the fibres (of yarn for this study), $E_m$ is Young's modulus of the matrix, and $V_f$ and $V_m$ are the volumetric fractions of the fibres and matrix, respectively. During this first stage, the matrix-fibre interface shear behaviour is assumed to be elastic. Stage I ends when the composite reaches the multiple cracking stress ($\sigma_{mc}$), which is the same as the first cracking stress (see Figure 10). This is calculated with the following formula:

$$\sigma_{mc} = \frac{E_I \sigma_{mu}}{E_m} \quad (2)$$

where $\sigma_{mu}$ is the tensile strength of the mortar. The strain at this point is calculated by

$$\varepsilon_I = \frac{\sigma_{mc}}{E_I} \quad (3)$$

When a crack appears in the matrix and reaches a fibre, debonding of the matrix-fibre interface occurs owing to weakness at this point. Then, a constant frictional interface

shear stress is assumed. This shear stress provides a normal stress transfer from the fibres to the inorganic matrix.

At the multiple cracking stage, distances between cracks are no shorter than the length of the debonded interface (δ) and no larger than 2δ. The spatial introduction of cracks occurs randomly until no space remains for new cracks, in a similar way to the geometrical car parking problem. Widom [34] determined that the average distance between cracks is X = 1.337δ. For this value, the composite strain at the end of stage II ($\varepsilon_{II}$) can be defined as

$$\varepsilon_{II} = (1 + 0.666\alpha_e)\frac{\sigma_{mu}}{E_m} \quad (4)$$

where

$$\alpha_e = \frac{E_m V_m}{E_f V_f} \quad (5)$$

In the third stage, only fibres contribute to bearing the stresses associated with the applied deformation. Thus, the matrix stress remains constant despite the increase in the tensile load. The FRCM stiffness at this stage is defined by the expression

$$E_{III} = E_f V_f \quad (6)$$

The tensile strength and Young's modulus of the fibres is defined by the experimental results of the yarn testing. Thus, the strain at the end of stage III ($\varepsilon_{III}$) is determined by

$$\varepsilon_{III} = \frac{A_f \sigma_f}{A_m E_{III}} - \frac{\sigma_{mc} + E_{III}\varepsilon_{II}}{E_{III}} \quad (7)$$

where $\sigma_f$ is the tensile strength of the fibres (the tensile strength of yarn for this study), $A_f$ is the sectional area of the fibres, and $A_m$ is the sectional area of the FRCM specimens.

### 5.1 Analytical model and comparison with experimental results

The ACK model is not applicable to FRCM with polyester-coated meshes because the low percentage of utilization of the polyester-coated meshes (see Table 6) may indicate a partial slipping within the FRCM. Thus, FRCM specimens which used epoxy-coated meshes are the most suitable candidates to be represented by the ACK model.

Table 7 summarizes the analytical results calculated with the ACK model and the results obtained with two variations of the ACK model, which are presented herein to improve its applicability to vegetal-fibre FRCM. In this table, the volumetric fraction of coated fibres ($V_{fr}$), volumetric fraction of mortar ($V_m$), mortar cracking stress ($\sigma_{cm}$), FRCM ultimate stress ($\sigma_u$), and Young's modulus at stage I ($E_I$) and stage III ($E_{III}$) of the trilinear model presented by ACK are listed. These parameters were calculated using equations (1) to (7).

**Table 7.** Analytical results of FRCM

| | **ACK Model** | | | | **Adjusted Model 1** | | | | **Adjusted Model 2** | |
|---|---|---|---|---|---|---|---|---|---|---|
| **Mesh** | Hemp | Flax | Sisal | Cotton | Hemp | Flax | Sisal | Cotton | Sisal | Cotton |
| **$V_{fr}$** | 0.014 | 0.014 | 0.078 | 0.067 | 0.014 | 0.014 | 0.078 | 0.067 | 0.078 | 0.067 |
| **$V_m$** | 0.986 | 0.986 | 0.922 | 0.933 | 0.986 | 0.986 | 0.922 | 0.933 | 0.922 | 0.933 |
| **$\sigma_{mc}$ (MPa)** | 4.82 | 4.80 | 4.45 | 4.33 | 4.82 | 4.80 | 4.45 | 4.33 | 3.33 | 3.25 |
| **$\sigma_u$ (MPa)** | 6.54 | 7.92 | 8.75 | 5.20 | 6.54 | 7.92 | 8.75 | 5.20 | 8.75 | 5.20 |

| | | | | | | | | | | |
|---|---|---|---|---|---|---|---|---|---|---|
| **$\varepsilon_{II}$ (%)** | 0.63 | 0.67 | 0.79 | 4.68 | 0.80 | 1.16 | 1.59 | 4.65 | 1.08 | 1.12 |
| **$E_I$ (GPa)** | 9.32 | 9.29 | 8.60 | 8.60 | 9.32 | 9.29 | 8.60 | 8.39 | 8.60 | 8.39 |
| **$E_{III}$ (GPa)** | 0.53 | 0.49 | 0.38 | 0.06 | 0.39 | 0.68 | 0.61 | 0.02 | 0.44 | 0.03 |

Noticeable differences between the experimental results and predictions made with the ACK model (see Figure 12) suggested that it should be modified. These poor fittings are mostly observed in stages II and III, where the ACK model predicts a stiffer response than the experimentally observed one.

In stage II, the ACK model was modified according the proposal made by Larrinaga et al. [35], which in turn was based on the equation of Eurocode 2 [36] to estimate the crack width ($w_k$) of reinforced concrete subjected to tensile forces:

$$wk = s_{r,max}(\varepsilon_{sm} - \varepsilon_{cm}) \quad (8)$$

where $s_{r,max}$ is the maximum crack spacing, $\varepsilon_{sm}$ is the mean strain in the reinforcement, and $\varepsilon_{cm}$ is the mean strain in the concrete between cracks.

It can be considered that the total addition of crack widths is equal to the difference between the elongation of the reinforcement and the elongation of the concrete:

$$\sum w = \Delta l - \Delta l_c = (\varepsilon_{sm} - \varepsilon_{cm}).\, l \quad (9)$$

The value of ($\varepsilon_{sm}$ - $\varepsilon_{cm}$) may be calculated from the following equation:

$$(\varepsilon_{sm} - \varepsilon_{cm}) = \frac{\sigma_s - k_t \frac{f_{ct,eff}}{\rho_{p,eff}}\left(1 + \alpha_e.\rho_{p.eff}\right)}{E_s} \quad (10)$$

where $\sigma_s$ is the stress of the reinforcement in a cracked section, $k_t$ is a factor dependent on the duration of the load, $f_{ct,eff}$ is the mean value of the tensile strength of the concrete at the time when the first crack is formed, $\rho_{p,eff}$ is the reinforcement ratio $A_s/A_c$, and $\alpha_e$ is the ratio $E_s/E_c$.

Equation (10) can be used to calculate the strain at the end of stage II. Adapting the notation to the FRCM system, the following expression is obtained:

$$\varepsilon_{II} = \frac{\sigma_u - k_t \frac{\sigma_{mc}}{\rho_{p,eff}}\left(1 + \alpha_{e2}.\rho_{p.eff}\right)}{E_f} - \varepsilon_I \quad (11)$$

where $\sigma_u$ is the tensile strength of the mesh, $\sigma_{mc}$ is the mean value of the tensile stress of the mortar at the time the first crack is formed, $\rho_{p,eff}$ is the reinforcement ratio $A_f/A_m$, and $\alpha_{e2}$ is the ratio $E_f/E_m$.

In Eurocode 2, the factor of the duration of the load ($k_t$) is equal to 0.6 for short-term loading and 0.4 for long-term loading. For our experiments, it is decided to use the value corresponding to short-term loads.

Stage III of the ACK model was also modified. This change was based on a formulation presented by Jimenez Montoya [37], which represents reinforced concrete using a polygonal law (N - ΔL/L), where it is assumed that the steel strain grows in parallel to the straight line of stage II (see Figure 11).

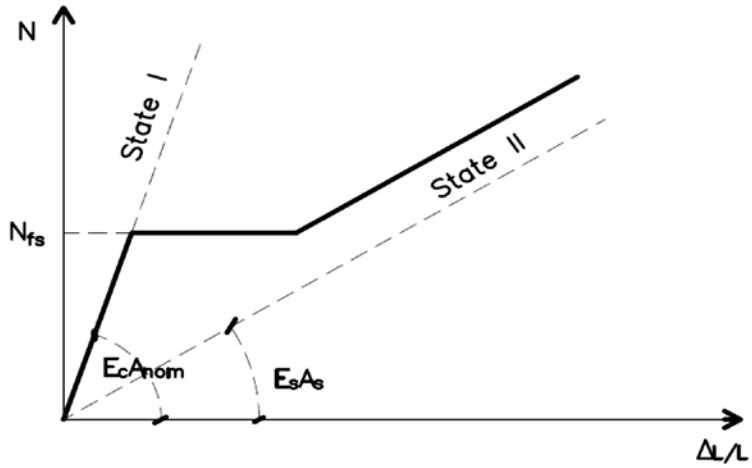


**Figure 11.** Theoretical behaviour of reinforced concrete [37]

In the implemented modified model ("adjusted model 1"), the strain at the end of stage III is calculated with the following equation:

$$\varepsilon_{III} = \frac{\sigma_u}{E_f V_f} \quad (12)$$

Young's modulus at stage III is

$$E_{III} = \frac{(\sigma_u - \sigma_{mc})}{(\varepsilon_{III} - \varepsilon_{II})} \quad (13)$$

In addition, it is observed that sisal and cotton FRCM showed lower cracking stress and lower strain at the end of stage II than that predicted by the ACK model or adjusted model 1 (see Figure 12). This fact can be attributed to the far lower modulus of elasticity of the coated sisal and coated cotton yarns (0.93 and 4.87 GPa, respectively) in comparison to the higher modulus of elasticity of the mortar matrix (8.92 GPa). Although the ratio between Young's modulus of the yarns and mortar was already considered in the equation, the authors considered it necessary to adjust equation (2) in order to represent the case of Young´s modulus of the mortar being far greater than the one of the yarns. In addition, the fitting between experimental and analytical results (Figure 12) supports this idea.

The second modification (adjusted model 2) was done to reduce the cracking stress value of FRCM ($\sigma_{mc}$). Equation (2) is multiplied by an empirical coefficient ($\beta$) set to 0.75 for cases in which Young's modulus of the fibres is lower than Young's modulus of the mortar.

$$\sigma_{mc} = \frac{\beta E_I \sigma_{mu}}{E_m} \quad (14)$$

In addition, the factor of duration of the load ($k_t$) was not considered in calculating the strain at the end of stage II ($\varepsilon_{II}$). This modification aimed to reduce $\varepsilon_{II}$ to improve the analytical fitting of cases in which Young's modulus of the fibres is lower than Young's modulus of the mortar.

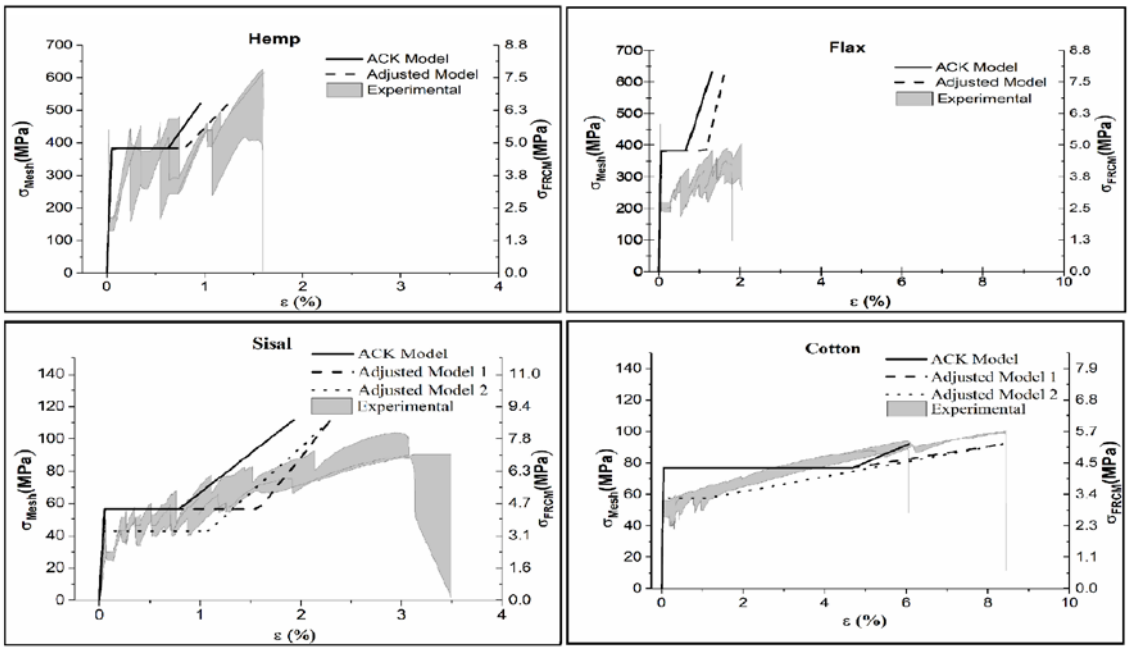


**Figure 12.** Contrast of experimental results with analytical models of FRCM

Experimental results, predictions of the ACK model, and predictions of the two adjusted models are shown together in stress-strain diagrams for comparison and analysis purposes.

Figure 12 shows that ACK model is not accurate at representing the tensile response of vegetal-fibre FRCM along the three stages. Moreover, neither ACK nor adjusted model 1 fit the experimental results obtained for flax FRCM specimens because these mostly failed owing to mortar detachment.

Nevertheless, ACK was suitable to model the structural response of the first stage (stage I) for cases in which Young`s modulus of the mesh was higher than Young's modulus of the matrix: hemp and flax FRCM. By contrast, adjusted model 2 predicts the cracking stress with better accuracy than the ACK model for cases in which Young`s modulus of the mesh was lower than Young's modulus of the matrix, thanks to considering the empirical coefficient (β).

All cases plotted Figure 12 show a progressive stress increase along multiple cracking formations (stage II). This does not fit the constant stress level proposed by the models for this stage. In addition, the strain range in which stage II develops is longer than that predicted by any model. These two particular differences are a result of the relative slip between fibres and mortar allowed by the clevis grips system (which is stronger than that with steel bars) and the nonlinear behaviour of the mortar [37].

In addition, the experimental stiffness degradation in stage III is greater than that of any model prediction. This may be caused by the discontinuous structure of vegetal fibre yarns and the progressive degradation of the fibres caused by the mesh-mortar local interaction.

According to Figure 12, the proposed modifications to the ACK model increase the accuracy when estimating the strains at the ends of stages II and III.

After analysing the results, it is highlighted that a correct mesh-matrix interaction is necessary to achieve the multiple cracking behaviour expected by FRCM and used as an initial hypothesis for the analytical models.

Therefore, this study confirms that the tensile behaviour of the FRCM is strongly influenced by the fibre-mortar volume ratio, the mesh-mortar adhesion, and the relationship between the mesh and matrix stiffness. Thus, an excessive number of fibres

can cause premature detachment of the mortar, and using a mesh with a Young's modulus lower than that of the matrix causes a reduction in the cracking stress.

## 6. Conclusions

Experimental tensile tests on coated vegetal-fibre FRCM were carried out. The results were compared with existing analytical models, and novel adaptations are proposed. The following conclusions are reached from this comprehensive research:

- The influence of the resin coating on the mechanical properties of yarns made of different materials mostly depended on the ability of the resin to penetrate its internal structure. This had special significance for yarns coated with polyester because this resin had lower fluidity than the epoxy resin.
- Resin coating increases the tensile strength and stiffness in almost all tested vegetal fibre yarns (except for sisal). It is of special significance in the case of hemp yarn, whose tensile strength and modulus of elasticity increased by 84% and 92%, respectively. Thus, it is necessary to apply an accurate control to the coating procedure to avoid altering the desired mechanical behaviour.
- FRCM with epoxy-coated mesh shows a greater percentage of utilization of the yarns than FRCM with polyester-coated mesh. This proves that epoxy resin has better compatibility with the mortar matrix than polyester.
- Coated-hemp FRCM reached the highest tensile strength, and coated-cotton FRCM made the greatest gain in developing a clear multicracking failure pattern.
- An excessive sectional area of yarns causes mortar debonding failure (see the sisal cases). Thus, the failure mode depends on the volume ratio between the fibres and the matrix, as well as the stiffness of the mesh.
- The tensions and multicracking failure reached by vegetal-fibre FRCM suggests that vegetal-fibre FRCM can reach mechanical properties that are comparable to (or even greater than) synthetic-fibre FRCM.
- The ACK model was not effective at predicting the behaviour of vegetal-fibre FRCM. The progressive increase in the stress along stage II is not considered by the ACK model, and the stiffness degradation is lower than that observed in experimental tests.
- The lower stiffness of the mesh in comparison with the matrix stiffness in the cases of sisal and cotton FRCM significantly affects the behaviour of the composite in stage I, causing a clear reduction in the tensile cracking stress.
- Adjusted analytical models proposed in this study exhibited better accuracy at predicting experimental responses than the ACK model. However, these analytical models were unable to model the progressive stress increase along stage II.

## Acknowledgements

The authors gratefully acknowledge the financial support from the Ministerio de Economía y Competitividad of the Spanish Government (MINECO) and the European Regional Development Fund (ERDF) through the MULTIMAS project (Multiscale techniques for the experimental and numerical analysis of the reliability of masonry structures, ref. num. BIA2015-63882-P). The first author also acknowledges the Ministry of Education Science and Technology (Mesyt) of the Dominican Republic for financial support through its international scholarship program. The authors gratefully

acknowledge the assistance of Dr. Christian Escrig and undergraduate students Marc Devos and Celina Camboni.

**References**

[1] E. Bernat-Maso, “Comportamiento estructural de muros de obra de fábrica reforzados con TRM,” in *Aplicaciones avanzadas de los materiales compuestos en la obra civil y la edificación*, no. 9, M. A. Perez, Ed. 2013, pp. 137–164.

[2] C. Escrig, L. Gil, and E. Bernat-Maso, “Experimental comparison of reinforced concrete beams strengthened against bending with different types of cementitious-matrix composite materials,” *Constr. Build. Mater.*, vol. 137, pp. 317–329, 2017.

[3] V. Alecci, F. Focacci, L. Rovero, G. Stipo, and M. De Stefano, “Intrados strengthening of brick masonry arches with different FRCM composites: Experimental and analytical investigations,” *Compos. Struct.*, vol. 176, pp. 898–909, 2017.

[4] V. Pino, A. Nanni, D. Arboleda, C. Roberts-Wollmann, and T. Cousins, “Repair of Damaged Prestressed Concrete Girders with FRP and FRCM Composites,” *J. Compos. Constr.*, vol. 21, no. 3, p. 4016111, 2016.

[5] A. Prota, G. Marcari, G. Fabbrocino, G. Manfredi, and C. Aldea, “Experimental In-Plane Behavior of Tuff Masonry Strengthened with Cementitious Matrix–Grid Composites,” *J. Compos. Constr.*, vol. 10, no. 3, pp. 223–233, 2006.

[6] C. Escrig, L. Gil, E. Bernat-Maso, and F. Puigvert, “Experimental and analytical study of reinforced concrete beams shear strengthened with different types of textile-reinforced mortar,” *Constr. Build. Mater.*, vol. 83, pp. 248–260, 2015.

[7] G. de Felice *et al.*, “Mortar-based systems for externally bonded strengthening of masonry,” *Mater. Struct.*, vol. 47, no. 12, pp. 2021–2037, 2014.

[8] O. A. Cevallos, R. S. Olivito, R. Codispoti, and L. Ombres, “Flax and polyparaphenylene benzobisoxazole cementitious composites for the strengthening of masonry elements subjected to eccentric loading,” *Compos. Part B Eng.*, vol. 71, no. April 2016, pp. 82–95, 2015.

[9] C. Rosamaria, “Mechanical Performance of Natural Fiber-Reinforced Composites for the Strengthening of Ancient Masonry,” University of Calabria, 2013.

[10] P. Wambua, J. Ivens, and I. Verpoest, “Natural fibres: Can they replace glass in fibre reinforced plastics?,” *Compos. Sci. Technol.*, vol. 63, no. 9, pp. 1259–1264, 2003.

[11] M. Ardanuy, J. Claramunt, and R. D. Toledo Filho, “Cellulosic fiber reinforced cement-based composites: A review of recent research,” *Constr. Build. Mater.*, vol. 79, pp. 115–128, 2015.

[12] H. Ahmad and M. Fan, “Interfacial properties and structural performance of resin-coated natural fibre rebars within cementitious matrices,” *Cem. Concr. Compos.*, vol. 87, pp. 44–52, 2018.

[13] F. Micelli and M. A. Aiello, “Residual tensile strength of dry and impregnated reinforcement fibres after exposure to alkaline environments,” *Compos. Part B Eng.*, 2016.

[14] J. Donnini and V. Corinaldesi, “Mechanical characterization of different FRCM systems for structural reinforcement,” *Constr. Build. Mater.*, vol. 145, pp. 565–575, 2017.

[15] T. D’Antino and C. Papanicolaou, “Mechanical characterization of textile reinforced inorganic-matrix composites,” *Compos. Part B Eng.*, vol. 127, pp. 78–91, 2017.

[16] C. Menna, D. Asprone, M. Durante, A. Zinno, A. Balsamo, and A. Prota, "Structural behaviour of masonry panels strengthened with an innovative hemp fibre composite grid," *Constr. Build. Mater.*, vol. 100, pp. 111–121, 2015.
[17] D. Snoeck, P. A. Smetryns, and N. De Belie, "Improved multiple cracking and autogenous healing in cementitious materials by means of chemically-treated natural fibres," *Biosyst. Eng.*, vol. 139, no. 1998, pp. 87–99, 2015.
[18] R. S. Olivito, O. A. Cevallos, and A. Carrozzini, "Development of durable cementitious composites using sisal and flax fabrics for reinforcement of masonry structures," *Mater. Des.*, vol. 57, pp. 258–268, 2014.
[19] O. A. Cevallos and R. S. Olivito, "Effects of fabric parameters on the tensile behaviour of sustainable cementitious composites," *Compos. Part B Eng.*, vol. 69, pp. 256–266, 2014.
[20] S. De Santis, F. G. Carozzi, G. de Felice, and C. Poggi, "Test methods for Textile Reinforced Mortar systems," *Compos. Part B Eng.*, vol. 127, pp. 121–132, 2017.
[21] F. G. Carozzi and C. Poggi, "Mechanical properties and debonding strength of Fabric Reinforced Cementitious Matrix (FRCM) systems for masonry strengthening," *Compos. Part B Eng.*, vol. 70, 2015.
[22] D. Arboleda, F. G. Carozzi, A. Nanni, and C. Poggi, "Testing Procedures for the Uniaxial Tensile Characterization of Fabric-Reinforced Cementitious Matrix Composites," *J. Compos. Constr.*, vol. 20, no. 3, p. 4015063, 2016.
[23] L. Ascione, G. De Felice, and S. De Santis, "A qualification method for externally bonded Fibre Reinforced Cementitious Matrix (FRCM) strengthening systems," *Compos. Part B Eng.*, vol. 78, pp. 497–506, 2015.
[24] G. P. Lignola *et al.*, "Performance assessment of basalt FRCM for retrofit applications on masonry," *Compos. Part B Eng.*, vol. 128, pp. 1–18, 2017.
[25] J. Hartig, F. Jesse, K. Schicktanz, and U. Häußler-Combe, "Influence of experimental setups on the apparent uniaxial tensile load-bearing capacity of Textile Reinforced Concrete specimens," *Mater. Struct. Constr.*, vol. 45, no. 3, pp. 433–446, 2012.
[26] D. Arboleda, "Fabric Reinforced Cementitious Matrix (FRCM) Composites for Infrastructure Strengthening and Rehabilitation : Characterization Methods," *PhD Thesis*, pp. 1–131, 2014.
[27] EN 1504-3, "EN 1504-3 Products and systems for the protection and repair of concrete structures - Definitions, requirements, quality control and evaluation of conformity - Part 3: Structural and non-structural repair," *http://www.aenor.es/*, 2005.
[28] UNE-EN 1015-11, "Métodos de ensayo de los morteros para albañilería - Parte 11: Determinación de la resistencia a flexión y a compresión del mortero endurecido," 2000, p. 14.
[29] BS EN ISO, "Textiles - Tensile properties of fabrics - Part 1: Determination of maximum force and elongation at maximum force using the strip method," no. EN ISO 13934-1/2, 2013.
[30] ICC Evaluation Service Inc., "Proposed Revisions to the Acceptance Criteria for Masonry and Concrete Strengthening Using Fiber-reinforced Cementitious Matrix (FRCM) Composite Systems, Subject AC434-0213-R1 (ME/BG)," 2012.
[31] D. Arboleda, "Fabric Reinforced Cementitious Matrix (FRCM) Composites for Infrastructure Strengthening and Rehabilitation : Characterization Methods," *PhD Thesis*, pp. 1–131, 2014.
[32] J. Aveston and A. Kelly, "Theory of multiple fracture of fibrous composites," *J. Mater. Sci.*, vol. 8, no. 3, pp. 352–362, Mar. 1973.

[33] P. Larrinaga, C. Chastre, H. C. Biscaia, and J. T. San-Jose, “Experimental and numerical modeling of basalt textile reinforced mortar behavior under uniaxial tensile stress,” *Mater. Des.*, vol. 55, pp. 66–74, 2014.
[34] B. Widom, “Random Sequential Addition of Hard Spheres to a Volume,” *J. Chem. Phys.*, vol. 44, no. 10, pp. 3888–3894, May 1966.
[35] P. Larrinaga, C. Chastre, J. T. San-José, and L. Garmendia, “Non-linear analytical model of composites based on basalt textile reinforced mortar under uniaxial tension,” *Compos. Part B Eng.*, vol. 55, pp. 518–527, 2013.
[36] BS EN 1992-1-1, “Eurocode 2: Design of concrete structures - Part 1-1 : General rules and rules for buildings,” *Br. Stand. Inst.*, vol. 1, no. 2004, p. 230, 2004.
[37] J. C. A. P. Alvaro Garcia Meseguer, Francisco Moran Cabré, *Jimenez Montoya - Hormigon Armado*, 15th ed. Barcelona, 2011.